ISSN 0016-7029, Geochemistry International, 2006, Vol. 44, No. 4, pp. 317–326. © Pleiades Publishing, Inc., 2006.
Original Russian Text © E.V. Sharkov, V.F. Smol'kin, V.B. Belyatskii, A.V. Chistyakov, and Zh.A. Fedotov, 2006, published in Geokhimiya, 2006, No. 4, pp. 355–364.

Age of the Moncha Tundra Fault, Kola Peninsula: Evidence from the Sm–Nd and Rb–Sr Isotopic Systematics of Metamorphic Assemblages

E. V. Sharkov*, V. F. Smol'kin, V. B. Belyatskii***, A. V. Chistyakov*, and Zh. A. Fedotov******

**Institute of the Geology of Ore Deposits, Petrography, Mineralogy, and Geochemistry, Russian Academy of Sciences, Staromonetnyi per. 35, Moscow, 119017 Russia*
e-mail: sharkov@igem.ru
***Vernadsky State Geological Museum, ul. Mokhovaya 11, korp. 2, Moscow, 125009 Russia*
****Institute of Precambrian Geology and Geochronology, Russian Academy of Sciences, nab. Makarova 2, St. Petersburg, 199034 Russia*
*****Geological Institute, Kola Scientific Center, Russian Academy of Sciences, ul. Fersmana 14, Apatity, Murmansk oblast, 184209 Russia*
Received June 2, 2004

Abstract—The first Sm–Nd and Rb–Sr dates were obtained for the dynamometamorphic processes associated with the origin and evolution of the Moncha Tundra fault, Kola Peninsula, which separates two large Early Paleoproterozoic layered intrusions: the Monchegorsk Ni-bearing mafic–ultramafic intrusion and the Main Range massif of predominantly mafic composition. The fault belongs to the regional Central Kola fault system, whose age was unknown. The material for the dating included metamorphic minerals from blastomylonitic rocks recovered by structural borehole M-1. Mineralogical thermobarometry suggests that the metamorphism occurred at 6.9–7.6 kbar and 620–640°C, which correspond to the amphibolite facies. The Sr and Nd isotopic systems were re-equilibrated, and their study allowed us to date the dynamometamorphic processes using mineral isochrons. It was established that the Moncha Tundra fault, and, respectively, the whole Central Kola fault system appeared in the middle of Paleoproterozoic ~2.0–1.9 Ga, simultaneously with the Svecofennian orogen in the central part of the region and the Lapland–Kola orogen in its northeastern part. Another episode of dynamometamorphism that occurred at 1.60–1.65 Ga is envisaged.

DOI: 10.1134/S001670290604001X

INTRODUCTION

The Monchegorsk area is of crucial importance for understanding the geology of the central part of the Kola region (Fig. 1). There are two large Early Paleoproterozoic layered intrusions separated by the large Moncha Tundra fault (Fig. 2): the Monchegorsk pluton of ultramafic (peridotite–pyroxenite) and mafic (gabbronorite) rocks (Moncha Pluton) and the Moncha–Chuna–Volch'i Tundras (Main Range), which are located west of the Monchegorsk pluton and are composed mainly of mafic rocks, dominated by gabbronorite–anorthosites [1, 2]. Both intrusions have autonomous internal structures, but differ in cumulate stratigraphy: the Moncha Pluton is dominated by ultramafic cumulates, whereas Main Range body consists mostly of mafic cumulates. The Main Range massif is broken into two massifs by faults: the Chuna–Volch'i Tundra and Moncha Tundra massifs.

The Moncha Tundra fault belongs to the regional Central Kola fault system, one of the major structures of the Lapland–Kola orogen (Fig. 1). However, the age of these faults is unconstrained as of yet. Our work was aimed at clarifying this problem, which is of great importance for understanding the geology of the Monchegorsk ore district and the entire Kola region. The method was based on the mineralogic and isotopic (Sm–Nd and Rb–Sr) study of metamorphic assemblages with the aim of determining the time when the isotopic systems closed and, respectively, when tectonic activity along the fault started to cease. The samples for this study were taken from the core of structural borehole M-1, which was drilled in the eastern slope of the Moncha Tundra Range on Mount Khipik, in the junction zone of the Main Range and Moncha Pluton (Fig. 2). The drilling was ordered by the Severonikel plant of the Kola Mining Company; the boreholes are described in [2].

STRUCTURE OF THE MONCHA TUNDRA FAULT

The Central Kola fault system extends northwest across the whole Kola Peninsula [3]. It separates the

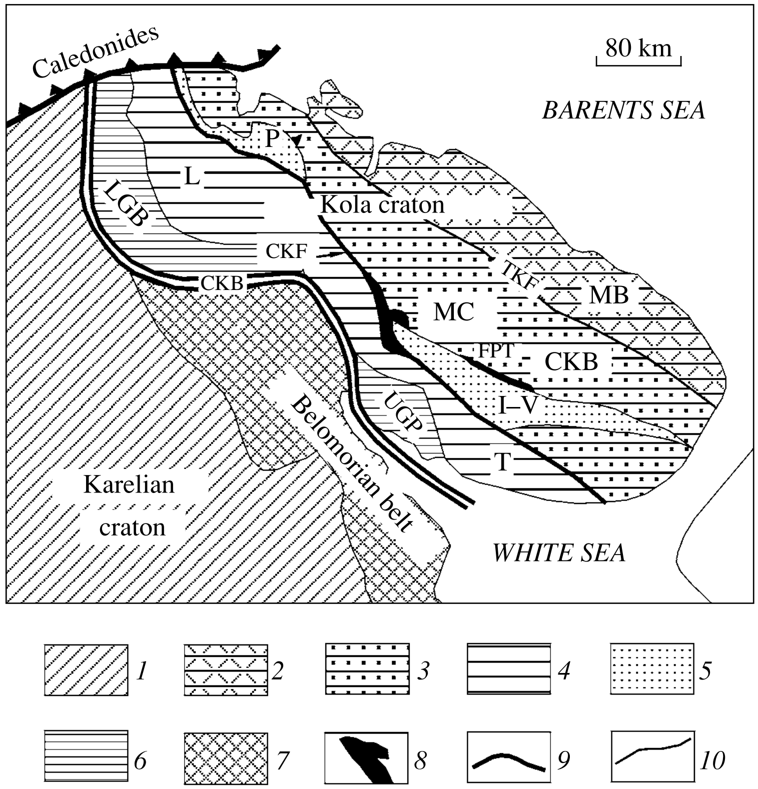

Fig. 1. Location of the Monchegorsk complex and major tectonic structures of the northeastern Baltic Shield. (*1*) Karelian craton; (*2–5*) Lapland–Kola orogen: (*2*) Murmansk block (MB); (*3*) Central Kola block (CKB); (*4*) Tersk–Lotta block ((T) and (L) Tersk and Lotta parts, respectively); (*5*) Pechenga–Varzuga volcanosedimentary belt ((P) and (I–V) Imandra–Varzuga structures, respectively); (*6*) Lapland–Umba granulite belt (LGB and UGB); (*7*) Belomorian mobile belt; (*8*) Early Paleoproterozoic mafic–ultramafic intrusions: (MC) Monchegorsk complex (Monchegorsk pluton and Main Range massif), (FPT) Fedorova–Pana Tundras; (*9*) Late Paleoproterozoic Central Kola fault (CKF); (*10*) other faults. (MLF) Main Lapland Fault.

northeastern part of the region (Central Kola and Murmansk blocks) from the southwestern part including the Tersk and Lotta blocks and Lapland–Umba granulite belt, as well as the Belomorian mobile zone. Geological data suggest that the fault system was formed during collision after the closure of the Svecofennian ocean and the formation of the orogen at 2.0–1.9 Ga. However, no isotope dates confirming this assumption were available.

Materials on the Moncha Tundra fault were used to date the dynamometamorphic processes caused by the tectonic displacements of the blocks along the Central Kola fault. In the study area, the fault is exposed in Pentlandite Canyon, where the fault has a width of ~1 km. The canyon exposes a great number of steep east-dipping normal–fault surfaces and a specific tectonic mixture of variable blastomylonitic intrusive rocks of both massifs, Archean gneisses, and mafic dikes of different age [2]. Structural borehole M-1 that was drilled through the western part of the Moncha Tundra fault entered the tectonic mixture at depths from 1000 to 2000 m (Fig. 3). The angle between the blastomylonite gneissosity and the core axis varies with depth from 0° to 45°–50°, showing a downward decrease in the dip of the fault zone. The mainly steep angles of the schistosity imply that the true thickness of the zone of blastomylonitization and cataclasis should be no more than 300–350 m.

GEOLOGY OF INTRUSIONS OF THE MONCHEGORSK COMPLEX

Intrusive rocks of the Monchegorsk Complex (Monchegorsk Pluton and Main Range Massif) are ascribed to the large early Paleoprotoerozoic Baltic igneous province of silicic high-Mg (boninitic) series, which developed over the eastern part of the Fennoscandian shield from ~2.55 to 2.3 Ga [4]. The province includes large layered mafic–ultramafic intrusions, gabbronorite dike swarms, and volcanosedimentary complexes in the riftogenic structures. One of the latter, the Pechenga–Varzuga belt in the Kola Peninsula, consists of the Pechenga and Imandra–Varzuga structural zones [5]. The intrusions considered in this paper are confined to the northwestern termination of the latter, which cuts across the Archean gneisses, amphibolites, granulites, and hypersthene diorites [2].

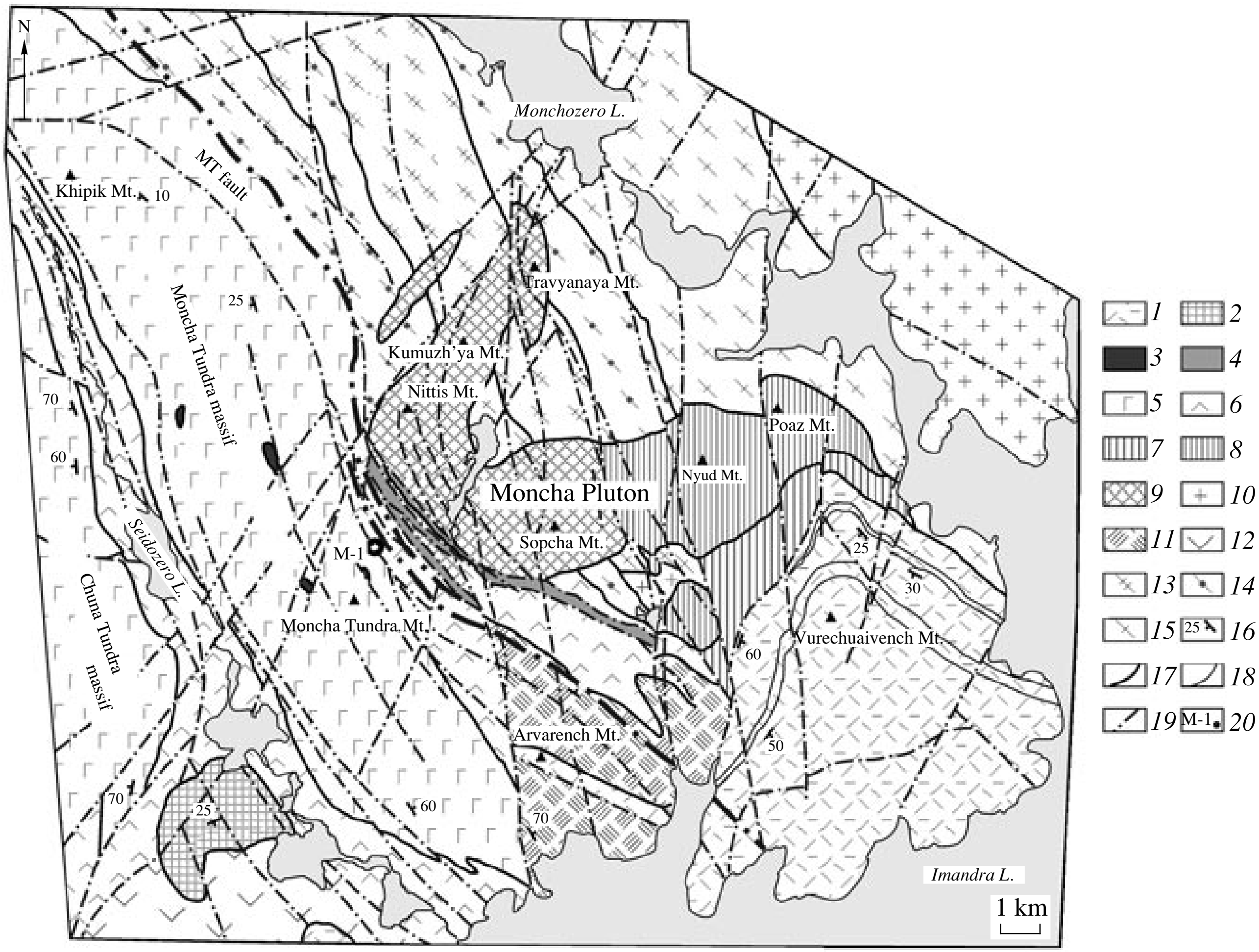

Fig. 2. Schematic geological map of the Monchegorsk area (modified after Smol'kin et al. [2]). (*1*) Metavolcanics, quartzites, and schists of the Paleoproterozoic Kuksha and Seidorechka formations of the Imandra–Varzuga structure; (*2*) ultramafics and gabbronorites of the Ostrovsk massif; (*3*) small troctolite intrusions; (*4*) large dike-shaped bodies of norites, orthopyroxenites, and gabbro; (*5–6*) Main Range massif: (*5*) gabbronorites and gabbronorite–anorthosites of the Moncha Tundra and Chuna Tundra massifs; (*6*) intercalation of blastomylonitic norites and orthopyroxenites, the same area; (*7–9*) Monchegorsk pluton: (*7*) metagabbro, gabbronorites, and anorthosites of the foothills of Vuruchuaivench Mount, (*8*) olivine norites, norites, gabbronorites (Nyud–Poaz Mounts), (*9*) orthopyroxenites, peridotites, and dunites (Nittis–Kumuzh'ya, Travyanaya, and Sopcha mounts); (*10–15*) Archean complex: (*10*) diorites, granodiorites, (*11*) acid volcanics, metasediments of Mount Arvarench, (*12*) schistose amphibolites of the Vitegubsk Formation; (*13*) high-Al gneisses; (*14*) garnet–biotite gneisses; (*15*) biotite–amphibole gneisses; (*16*) dip and strike (orientation of trachytic textures or bedding); (*17*) geological boundaries; (*18*) traced horizons within the Imandra–Varzuga structure; (*19*) tectonic faults (position of the axial part of the Moncha Tundra (MT) fault is shown by bold); (*20*) borehole M-1.

The two models for the geological relations between the intrusions that were the most popular in the 1960s–1980s are as follows. One of them [6, 7] suggested that the Main Range massif was formed in the Late Archean, while the Moncha pluton formed at the end of the Early Proterozoic, after the deposition and metamorphism of the Early Proteorozic volcano-sedimentary rocks of the Imandra Varzuga zone. The other model, which was proposed by one of the authors, assumed that the gabbroanorthosites continued the common Moncha Pluton sequence and, therefore, can be combined in the single Monchegorsk (Moncha Tundra) complex [8]. According to recent geological–petrological data, the intrusions presumably belong to two independent bodies, generated by similar melts of the silicic high-Mg series [1, 2].

By now numerous U–Pb and Sm–Nd geochronological dates have been obtained for the magmatic rocks of the Monchegorsk region [2, 9–12]. According to these data, the Monchegorsk pluton was formed from 2507 ± 9 to 2493 ± 7 Ma (U–Pb zircon and baddeleyite dates). The large mafic dikes cutting through ultramafic rocks in the western part of the Moncha Pluton are similar in age (2506–2487 Ma) [2]. Rocks from the Main Range yield different dates. Zircons from three unaltered samples in the eastern slope of Mount Moncha Tundra define a narrow range from 2505 ± 6 to 2501 ± 8 Ma, while the gabbroanorthosites from the Chuna Tundra

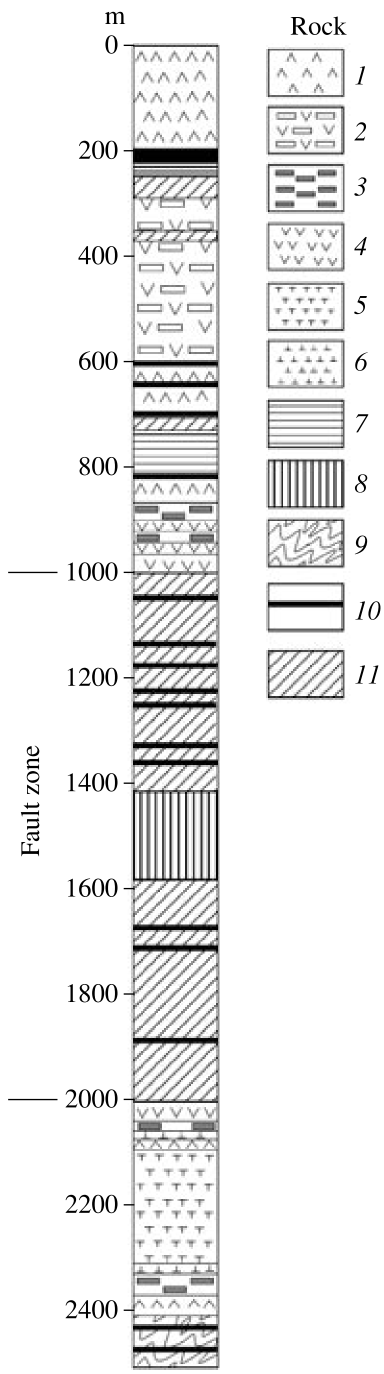

Fig. 3. Schematic vertical section constructed on the basis of materials recovered by structural borehole M-1. (*1*) Gabbronorite–anorthosites (*Pl* cumulates); (*2*) gabbronorites (*Pl* + *Px* cumulates); (*3*) bronzitites (*Opx* cumulates); (*4*) norites (*Pl* + *Opx* cumulates); (*5*) harzburgites (*Ol–Crt–Opx* cumulates); (*6*) dunites (*Ol–Crt* cumulates); (*7*) zones of thin intercalation of mafic and ultramafic rock; (*8*) blastocataclased Archean gneisses and diorites from the tectonic block; (*9*) underlying Archean gneisses and diorites; (*10*) dolerite dikes; (*11*) tectonic mixture of blastomylonitic gabbroids in the fault zone.

massif gave 2467 ± 7 Ma [2]. Previous dates for the rocks of Mount Moncha Tundra of 2453 ± 4 Ma [11] are presumably underestimates. In general, available data presumably indicate the close in time formation of the rocks of the Moncha pluton and the Main Range massif.

At the end of Early Paleoproterozoic, the upper part of the Moncha Pluton was subsequently eroded, overlain by conglomerates, and later by volcanic rocks composing the western flank of the Imandra–Varzuga riftogenic structure. The U–Pb zircon age of acid volcanic rocks is 2448 ± 8 Ma, while the gabbroids of the Imandra Complex cutting across them define U–Pb zircon and baddeleyite ages within 2442–2437 Ma [2]. These events produced numerous dolerite dikes cutting through both the Moncha Pluton and the Main Range massif.

Structure of the Intrusive Bodies

The Monchegorsk pluton (Fig. 2) is a typical layered intrusion, hosting deposits and occurrences of the sulfide Cu–Ni, chromite, and PGE ores [2, 6, 8, 13]. It is arc-shaped in plan view and consists of two branches: a northeastern branch, which is seven km long and composes the mounts of Nittis, Kumuzh'ya, and Travyanay (or NKT), and an eastern branch, which is nine km long and includes mounts Sopcha, Nyud, and Poaz. Each of them has a basin-shaped morphology and autonomous internal structure with subhorizontal layering in the internal zone. Both branches dip southwest, toward the Main Range massif, where their thickness increases.

From bottom to top, the quartz-bearing norites and gabbronorites of the endocontact (near-bottom) zone, 10–100 m thick, grade into the Peridotite zone, which consists of the olivine–chromitite cumulates (dunites and poikilitic harzburgites) 100–200 m thick in the lower part and is made up of rhythmically alternating olivine–chromite, olivine–orthopyroxene, and orthopyroxene cumulates (harzburgites and orthopyroxenites) 250–400 m thick in the upper zone. There rocks are followed by the Pyroxenite zone of orthopyroxene cumulates, 300–700 m thick. The uppermost part of the pluton comprises plagioclase–orthopyroxene cumulates, which are eroded in the eastern part of the pluton, at mounts Nyud and Poaz, as well as in the foothills of Mount Vuruchuaivench.

The Moncha Pluton mostly shows no significant alteration, with the only exception of its southeastern part, which is overlain by volcanosedimentary rocks of the Imandra–Varzuga Zone. The norites and gabbronorites experienced intense alterations under greenschist facies conditions, whose intensity increases outward.

The Main Range massif extends submeridionally for 80 km at a width from 1–2 to 15–20 km and has an area of ~440 km^2 [1, 3, 7]. A submeridional fault cuts the intrusion into two tectonic blocks, which are often referred to as separate massifs: the more extended Chuna Volch'i Tundra massif and the smaller Moncha Tundra massif, with a narrow band of Archean gneisses and amphibolites hosting the small Ostrovsk mafic–ultramafic intrusion in between (Fig. 1). The Main Range intrusion is presumably a differentiated lopolith [1, 7]. Its internal structure was disturbed by listric faults, which grade into low-angle E- and SE-dipping overthrusts, and by transverse subvertical normal faults.

The integral vertical section of the exposed rocks of the Main Range can be subdivided into three zones, varying in the vertical section from gabbronorites to gabbronorite–anorthosites [8]. The lowermost gabbronorite zone, 500–600 m thick, consists of gabbronorites at flanks and rhythmical alternation of predominant gabbronorites with olivine gabbronorites, pyroxenites, and plagioperidotites in the central part. The middle, gabbronorite–anorthosite zone from 0.3–0.5 km (Volch'i Tundra) to 2–2.5 km (Moncha Tundra) thick, mainly consists of trachytoid gabbronorite–anorthosites no less than 2.5–3 km thick. The overlaying rocks were eroded.

The Main Range massif is cut by small clinopyroxenite–wehrlite intrusions (Rainechorr, Kerkchorr, and others), lenslike bodies of melanocratic troctolites (harrisites), and later dikes of dolerites, ferrodolerites, and ferropicrites varying in thickness and length. The gabbroids were unevenly metamorphosed to the amphibolite facies, with the most intense metamorphism confined to the tectonic zones and their vicinities. The main process was the replacement of mafic minerals by amphibole, green hornblende; the dislocation zones proper often contain the garnet–amphibole metamorphic assemblage.

The lower and middle parts of the Main Range massif (Moncha Tundra) were penetrated by deep structural borehole M-1, briefly described below.

Vertical-Section Penetrated by Structural Borehole M-1

Structural borehole M-1 was started at the foot of the eastern slope of the Moncha Tundra Massif and drilled to a depth of 2500 m to penetrate the vertical section of the Moncha Tundra Massif and to confirm the presence of mineralized rocks beneath it (this hypothesis was invalidated). In spite of the fact that the rocks are strongly tectonized and the sequence is disturbed, the available material allowed us to decipher the structure and composition of the massif. As is seen in Fig. 3, the thick gabbronorite zone overlays rhythmically alternating gabbronorites, olivine gabbronorites, norites, and orthopyroxenites with single thin interbeds of dunites and harzburgites. They grade downward into gabbronorites and gabbronorite–anorthosites, which are separated by thick zones of schistosity and blastomylonitization. The thickest zone was found at depths from 1400 to ~ 1600 m; its middle part contains a tectonic block of Archean plagiogneisses and hypersthene diorites, which experienced intense cataclasis, mylonitization, and blastesis. In the interval of 2037–2387 m, the borehole penetrated plagioharzburgites, norites, and orthopyroxenites, which compose an independent intrusive body according to [2]. A thin outer contact zone, 37 m thick, composed of orthopyroxenites, gabbronorites, and chlorite–actinolite schist after them was found at the contact with the underlying aluminous gneisses of the Kola Group. The underlying rocks are highly silicified cataclased garnet–two-mica and garnet–amphibole plagiogneisses, as well as cordierite–hypersthene schists and diorites.

The borehole penetrated numerous partly cataclased dikes of different composition and thickness. They are composed of olivine gabbronorites, micronorites, microgabbros, and high-Ti dolerites [2] and cut the Moncha Tundra rocks and plagiogneisses to a depth of 1710 m. The number of the large dikes is equal to ten, and their total thickness is 65 m.

The fault zone in borehole M-1 looks like a tectonic mixture of cataclased Archean gneisses and diorites, and blastomylonitic gabbroids and ultramaic rocks including rocks of dike complexes of different ages. The thickness of cataclased rocks is as large as 1000–1200 m, i.e., accounts for half of the vertical section crossed by the borehole (Fig. 3). The zone experienced uneven brecciation and blastesis, but the rocks preserve their primary appearance at separate intervals and allow the reconstruction of their primary nature.

SAMPLE DESCRIPTION

We selected six samples of our collection from borehole M-1, and three of them were analyzed (sample number corresponds to the depth).

(1) Sample 1088.0 m is blastomylonitic silicified metagabbroanorthosite (plagioclase cumulate) composed of saussuritized plagioclase, green hornblende, garnet, and quartz. In spite of the complete replacement of magmatic minerals, relicts of primary cumulate textures remain occasionally preserved in places. Silicification occurs as fine veinlets and lenses of granulated quartz. The rock has the following mineral composition (in vol %): plagioclase 51, quartz 26, green hornblende 12, garnet 6, Ti-magnetite 4, carbonate 1, biotite and apatite < 1.

(2) Sample 1997.7 m is cataclased garnet–two-mica plagiogneiss, it is presumably, a fragment of the Archean complex found as a tectonic wedge in the middle part of the section. The texture is cataclastic, augen. Mineral composition is as follows (in vol %): moderate-Ca plagioclase 55, quartz 24, garnet 5, biotite 6, muscovite 4, staurolite 1, chlorite 1, apatite, Ti-magnetite, and sulfides.

(3) Sample 2388.8 m is Archean cataclased plagiogneiss with garnet and hornblende, which intercalates

Table 1. Contents of major (wt %) and trace (ppm) elements in the garnet-amphibolite blastomylonite (sample M1/1088.0) based on ICP-MS analysis

SiO_2	60.43	As	1.3	In	0.05	U	0.88
TiO_2	1.75	Ba	330	Mo	2.95	V	466
Al_2O_3	15.93	Co	26.2	Nb	6.34	W	1.32
Fe_2O_3	11.46	Cr	108	Ni	44.5	Y	16.8
MnO	0.13	Cs	0.62	Pb	7.59	Zn	82.5
MgO	2.05	Cu	47.3	Rb	26.3	Zr	123
CaO	5.69	Ga	20.3	Sn	2.41		
Na_2O	2.71	Ge	1.29	Sr	299		
K_2O	0.59	Hf	3.51	Ta	0.49		
P_2O_5	0.18	Ho	0.575	Th	5.60		
Total	100.92						

with high-Al hypersthene–cordierite crystalline schists. Rock texture is taxitic, from fine to medium-grained, blastoporphyritic. The mineral composition (in vol %): moderate-Ca plagioclase 89, quartz 5, garnet 3, hornblende 2, epidote 1, biotite < 1, sulfide < 1.

Cataclased silicified metagabbroanorthosite (sample 1088) was taken to solve the problem formulated above, since the U–Pb age of the Moncha Tundra Massif is known to be 2501 ± 8 Ma [2], while cataclasis was related to the main tectonic event, directed along the Moncha Tundra fault. These rocks are widespread in the fault zone and consist of a prograde metamorphic garnet–hornblende assemblage that developed immediately after primary magmatic minerals. The absence of fibrous actinolite and chlorite, which are often present in other samples of blastomylonites after gabbroids from the fault zone, presumably indicates that the rock was not affected by diaphthoresis under green-schist facies conditions. The chemical composition of the rock is presented in Table 1.

The REE distribution pattern is shown in Fig. 4. The relatively high LREE contents, the typical absence of Eu anomaly [2], as well as the elevated contents of SiO_2 and Zr, indicate that the chemical composition of the gabbronorites were not significantly modified during dynamometamorphism. Such alterations were presumably related to the influx of granitizing fluids in the fault zone, which is confirmed by the presence of granophyre veins.

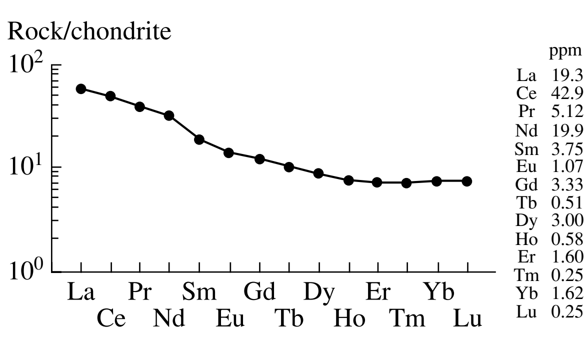

Fig. 4. Chondrite-normalized REE distribution pattern in sample M1/1088.

Monomineralic fractions of garnet, amphibole, and plagioclase were preliminarily studied on a microprobe (Table 2). Garnet in sample 1088.0 is almandine with an iron mole fraction (*f*) varying within a narrow range of 85.3 to 90.3 (at %). Separate grains show zoning: MnO decreases from core to rim (respectively, 2.67–2.46 and 0.52 wt %) at a similar iron mole fraction, which confirms a prograde evolution of the dynamometamprhic processes. The amphibole is a Fe–Ca variety, with *f* (at %) varying from 58.7 to 63.0, and can be ascribed to ferrotschermakite according to the Leake classification. Biotite coexisting with amphibole is dominated by a high-Ti variety (1.30–2.00 wt % TiO_2) with *f* (at %) from 46.6 to 53.5. Biotite with low TiO_2 contents (up to 0.5–0.6 wt %) is less common. The metamorphic plagioclase corresponds to andesine–labradorite with 50.0–55.6% *An*. In addition, the rock contains relicts of $An_{76.8}$, which are overgrown and replaced by lower-Ca plagioclase $An_{44.5–48.4}$.

Isotopic investigations were performed at the Institute of Precambrian Geology and Geochronology, Russian Academy of Sciences, on a Finnigan MAT-261 eight-collector mass spectrometer. The results of the Sm–Nd and Rb–Sr isotopic analyses are shown in Table 3.

DISCUSSION AND CONCLUSIONS

Mineralogic thermobarometry on the metamorphic assemblage garnet (*Gr*)–hornblende (*Hbl*)–plagioclase (*Pl*)–quartz (*Qtz*) defined the following metamorphic parameters: 6.9–7.6 kbar (by the *Pl* + *Hbl* + *Gr* + *Qtz* geobarometer [14] and 620–640°C (by the *Pl* + *Hbl* + *Gr* + *Qtz* geothermometer [15]), which correspond to the amphibolite facies. Under these conditions, the Sr and Nd isotopic systems in the rocks must have been reequilibrated. Correspondingly, the newly formed minerals acquired new isotopic signatures, which defined mineral isochrons yielding the age of dynamometamorphism. The relatively high pressure estimates are presumably related to stresses during the formation of metamorphic assemblages in the fault zones and can hardly reflect the depth of the process.

As is seen from the aforesaid data, the Sm–Nd dates are 100–150 Ma older than the Rb–Sr dates (Figs. 5–10), which can be related to the lower closure temperature of the Rb–Sr systems and possibly characterizes the duration of that tectonic episode. In particular, blastocataclasis and metamorphism of the metagabbroanorthosites of the Moncha Tundra massif of the Main Range is dated at 2038 ± 58 Ma by the Sm–Nd method

Table 2. Chemical composition of minerals from metamorphic assemblage in the garnet-amphibole blastomylonite (sample M1/1088) based on microprobe analysis

Phase	*Gr*	*Gr*	*Gr*	*Amf*	*Amf*	*Amf*	*Bi*	*Bi*	*Pl*	*Pl*	*Pl*
No.	20	7-c	7-r	1	23	8	17	11	29	3b	10b
SiO_2	37.61	36.93	36.80	40.24	40.94	39.70	35.26	35.01	54.60	53.69	48.19
TiO_2					0.24	0.26	1.58	0.30			
Al_2O_3	20.77	21.14	20.94	17.25	16.73	16.72	16.44	19.21	26.59	26.84	31.75
FeO	29.60	29.05	31.63	18.17	18.42	18.52	18.68	19.51	0.00	0.02	0.00
MnO	0.86	2.46	0.53	0.06	0.02	0.05	0.02	0.01			
MgO	2.77	2.32	2.24	6.86	6.63	6.33	11.90	9.53			
CaO	6.19	6.77	5.70	11.10	11.50	11.21	0.05	0.15	9.25	10.70	16.22
Na_2O					1.12	1.30	0.15	0.29	5.16	4.71	2.72
K_2O					0.34	0.26	9.03	9.38	0.03	0.05	0.01
Total	97.80	98.67	97.84	93.68	95.94	94.35	93.11	93.39	95.63	96.01	98.89
f, at %	85.7	87.5	88.8	59.8	60.9	62.1	46.8	53.5			
An, %									50	56	77

Note: (*Gr*) garnet [(20) large porphyroblast intergrown with amphibole; (7) small zoned crystal: c – core, and r – rim]; (*Amf*) amphibole [(1) large grain intergrown with quartz; (23) amphibole intergrown with garnet; (8) small amphibole grain near garnet]; (*Bi*) biotite [(17) biotite together with quartz enclosed in garnet; (11) biotite enclosed in plagioclase], (*Pl*) plagioclase [(29) plagioclase replaced by mica, at the contact with garnet; (3b) large plagioclase intergrown with quartz; (10b) large heterogeneous grain of relict plagioclase intergrown with amphibole and quartz replaced by low-Ca phase].
Microprobe analyses were conducted at the Geological Institute of the Kola Scientific Center, Russian Academy of Science, Apatity.

Table 3. Results of isotopic investigations of minerals and rocks from the core of borehole M-1

Sample	[Sm]	[Nd]	$^{147}Sm/^{144}Nd$	$^{143}Nd/^{144}Nd$	2σ	ϵ	[Rb]	[Sr]	$^{87}Rb/^{86}Sr$	$^{87}Sr/^{86}Sr$	2σ
Ml/1088											
WR	11.25	71.07	0.09555	0.511503	14	1.19	27.09	291.4	0.26906	0.711184	26
Amf	3.641	20.9	0.10565	0.511625	16	–14.4	24.1	189	0.36952	0.713821	28
Pl	2.345	23.25	0.06117	0.511052	18	2.13	6.079	120.6	0.14586	0.707659	22
Gr	1.663	6.404	0.15752	0.512344	18	6.98	2.096	14.54	0.41743	0.715119	20
Ml/2388.8											
WR	9.214	57.83	0.09661	0.510612	15	–18	53.37	312.6	0.49446	0.721338	19
Pl	9.378	62.75	0.09063	0.510565	9	–14.6	2.16	977.1	0.0064	0.710245	21
Gr	9.051	32.45	0.16916	0.511411	16	–27.2	6.652	70.2	0.27494	0.716458	22
Ml/1197.7											
WR	4.017	18.41	0.13232	0.511251	13	–11.4	70.51	383.3	0.53308	0.723925	25
Pl	3.643	41.7	0.05298	0.510315	12	6.06	3.156	732.7	0.01247	0.711628	27
Gr	12.56	30.18	0.2524	0.512694	19	–12.6	4.649	2073	0.0065	0.721227	24

Note: ε_{Nd} (1900 Ma) was calculated relative to the chondrite uniform reservoir (CHUR): $^{147}Sm/^{144}Nd = 0.1967$, $^{143}Nd/^{144}Nd = 0.512638$, $(^{87}Sr/^{86}Sr)t$ is the initial Sr isotope composition at t = 1900 Ma.

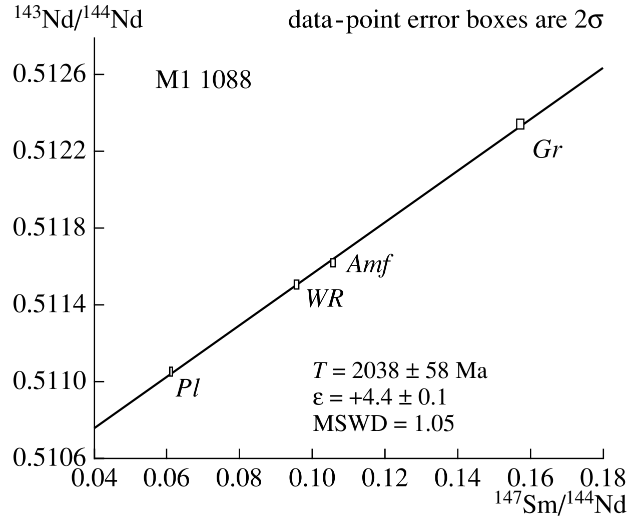

Fig. 5. Sm–Nd isochron for sample M1/1088. Hereinafter (Figs. 6–10): (*Pl*) plagioclase, (*Amf*) amphibole, (*Gr*) garnet, (*WR*) whole rock.

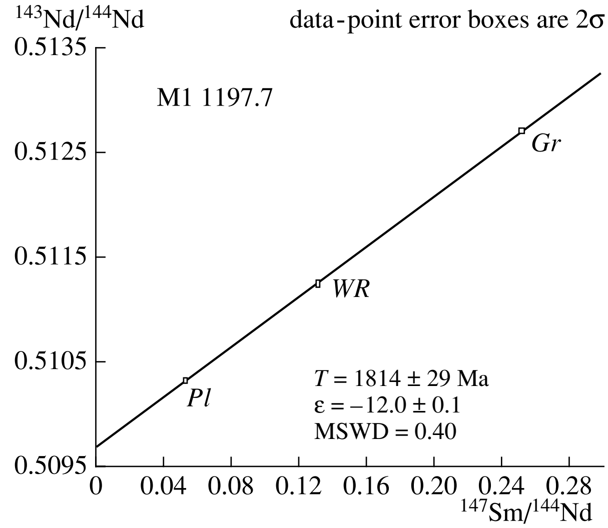

Fig. 6. Sm–Nd isochron for sample M1/1197.5

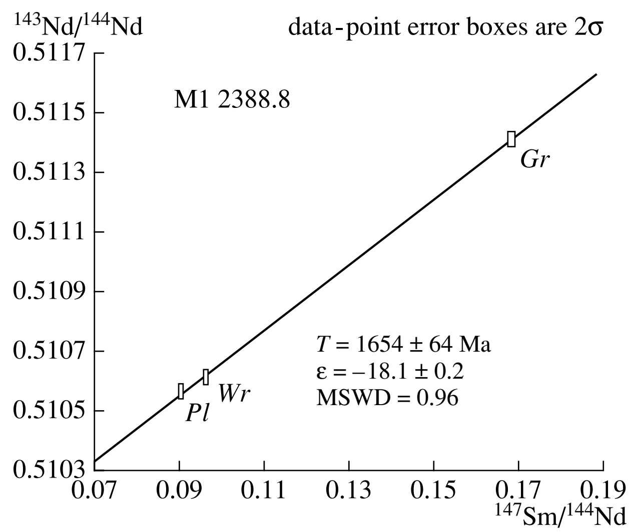

Fig. 7. Sm–Nd isochron for sample M1/2388.8.

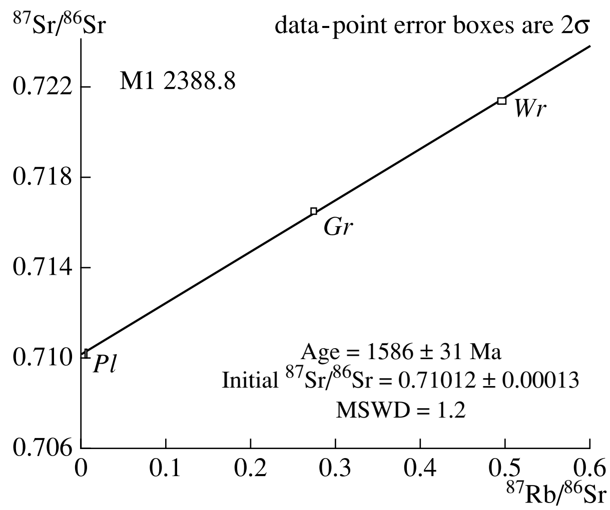

Fig. 8. Rb–Sr isochron for sample M1/1088.0.

and 1908 ± 52 Ma by the Rb–Sr method. These values indicate that the formation of the fault was related to the Svecofennian events. The $^{87}Sr/^{86}Sr$ ratio of this rock is 0.70370, which is well consistent with the mantle origin of protolith. At the same time, εNd (1900) of + 4.4 is not typical of the studied rocks of the Moncha Pluton and Moncha Tundra massif, whose εNd(2500) typically varies from –1 to –2 [2]. It is possible that the change in the Nd signatures was caused by the influence of the granitizing fluids, which penetrated the fault zone during dynamometamorphism.

A younger age was found for cataclased Archean rocks: their Rb–Sr dates are 1644 ± 31 and 1586 ± 31 Ma. They are nearly overlapped in the extreme values, giving an average age of 1610 Ma. The $^{87}Sr/^{86}Sr$ ratios in these rocks principally differ from the previous ones and are, respectively 0.71133 and 0.71012, indicating crustal signatures of the protoliths. The gneisses have somewhat different Sm–Nd dates: 1814 ± 29 and 1654 ± 64 Ma at εNd = –12.0 and –18.1, respectively. The age of the garnet–plagioclase plagiogneisses is close to the aforementioned value, whereas that for the garnet–two-mica gneisses is significantly younger and much older than those of the metagabbroanorthosites and lies in between. The values of εNd in the gneisses are relatively similar, and their strong negative values suggest a crustal protolith.

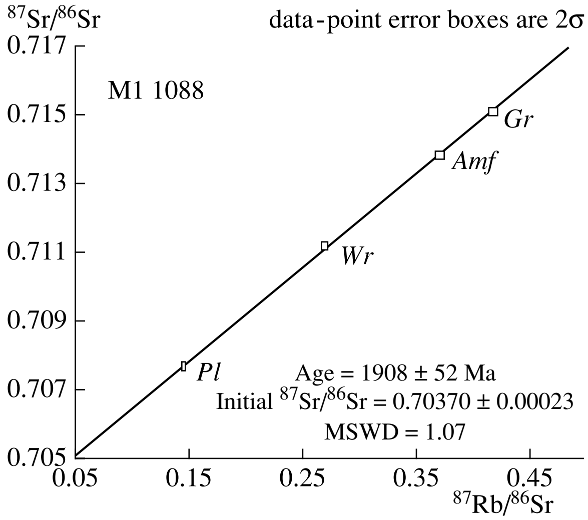

Fig. 9. Rb–Sr isochron for sample M1/1197.5.

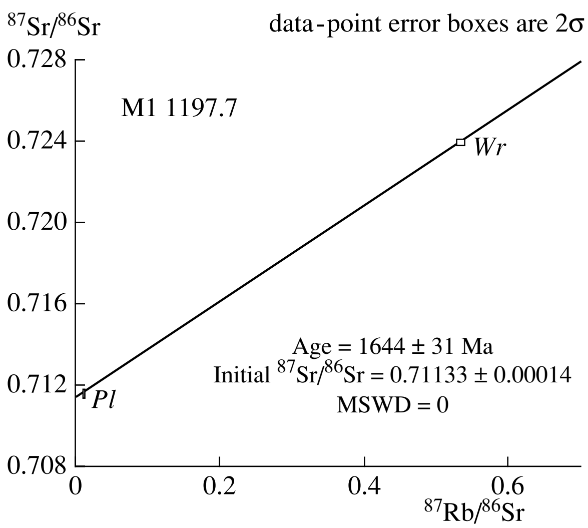

Fig. 10. Rb–Sr isochron for sample M1/2388.8.

The following conclusion can be drawn from our data: the Moncha Tundra fault, as the entire Central Kola fault system, evolved for a long time. Its appearance at 2.0–1.9 Ga coincided with the formation of an orogen at the site of the Svecofennian ocean in the central part of the Baltic shield and the formation of the Lapland–Kola orogen, including this fault, in its northeastern rear part.

In addition, another episode likely occurred at ~1.60–1.65 Ga in the evolution of the fault. Analogous dates were previously determined by the U–Pb zircon method for some lower-crustal xenoliths from the volcanic pipe of Elovy island (Kandalaksha Archipelago in the White Sea) [16]. This age correspondence can hardly be a mere coincidence, since large volumes of anorthosite–rapakivi granites were emplaced at that time in the Svecofennian block bordering on the Kola region in the southwest. We believe that this event has left its traces in the Kola region, but this stage of its evolution remains still poorly studied.

ACKNOWLEDGMENTS

We are grateful to A.S. Galkin and A.N. Dedyukhin, the heads of the Geological Survey of the Severonikel plant of the Kola Mining Company in Monchegorsk, for help in this work. The study was supported by the Russian Foundation for Basic Research (Project no. 04-05-64581) and the International Foundation RFBR–CNRS (French) (project No. 01-05-22001).

REFERENCES

1. E. V. Sharkov, V. F. Smolkin, A. V. Chistyakov, et al., "Geology and Metallogeny of the Monchegorsk Layered Complex," in *Russian Arctic. Geological History, Minerageny, and Geoecology*, Ed. by D. A. Dodin and V. S. Surkov (VNIIOkeanologiya, St. Petersburg, 2002), pp. 485–494 [in Russian].
2. V. F. Smolkin, Zh. A. Fedotov, Yu. N. Neradovskii, et al., *Layered Intrusions of the Monchegorsk Ore District: Petrology, Mineralization, Isotopic Compositions, and Deep-seated Structure* (Kolsk. Nauch. Ts. Ros. Akad. Nauk, Apatity, 2003), Vol. 2 [in Russian].
3. *1 : 500 000-Scale Geological Map of the Kola Region, Northeastern Part of the Baltic Shield*, Ed. by F. P. Mitrofanov (Kolsk. Nauch. Ts. Apatity, 1996) [in Russian].
4. E. V. Sharkov, V. F. Smolkin, and I. S. Krassivskaya, "Early Proterozoic Igneous Province of Siliceous High-Mg Boninite-like Rocks in the Eastern Baltic Shield," Petrologiya **5** (5), 503–522 (1997) [Petrology **5** (5), 448 (1997)].
5. E. V. Sharkov and V. F. Smolkin, "The Early Proterozoic Pechenga–Varzuga Belt: A Case of Precambrian Back-Arc Spreading," Precambrian Res. **82**, 133–151 (1997).
6. E. K. Kozlov, B. A. Yudin, and V. S. Dokuchaeva, *Mafic and Ultramafic Complexes of the Moncha–Volchi Tundras* (Nauka, Leningrad, 1967) [in Russian].
7. B. A. Yudin, *Gabbro–Labradorite Formation of the Kola Peninsula* (Nauka, Leningrad, 1980) [in Russian].
8. E. V. Sharkov, *Petrology of Layered Intrusions* (Leningrad, 1980) [in Russian].
9. I. N. Tolstikhin, V. S. Dokuchaeva, I. L. Kamensky, and Yu. A. Amelin, "Juvenile Helium in Ancient Rocks: II. U–He, K–Ar, Sm–Nd and Rb–Sr Systematics in the Monche Pluton. $^{3}He/^{4}He$ Ratios Frozen in Uranium-Free Ultramafic Rocks," Geochim. Cosmochim. Acta **56**, 987–999 (1992).
10. Yu. A. Balashov, T. B. Bayanova, and F. P. Mitrofanov, "Isotope Data on the Age and Genesis of Layered Intrusions in the Kola Peninsula and Northern Karelia, Northeastern Baltic Shield," Precambrian Res. **64** (1–4), 197–205 (1993).

11. F. P. Mitrofanov, V. V. Balaganskii, Yu. A. Balashov, et al., "U–Pb Age of Gabbro–Anorthosites of the Kola Peninsula," Dokl. Akad. Nauk **331** (1), 95–98 (1993).
12. Yu. V. Amelin, L. M. Heaman, and V. S. Semenov, "U–Pb Geochronology of Layered Intrusions in the Eastern Baltic Shield: Implications for the Timing and Duration of Paleoproterozoic Continental Rifting," Precambrian Res. **75**, 31–46 (1995).
13. G. I. Gorbunov, Yu. N. Yakovlev, Yu. V. Goncharov, et al., "Ni-bearing Districts of Kola Peninsula," *Copper–Nickel Deposits of the Baltic Shield*, Ed. by G. I. Gorbunov and Kh. Pappunen (Nauka, Leningrad, 1985) [in Russian].
14. M. Y. Kohn and F. S. Spear, "Two New Geobarometers for Garnet Amphibolites, with Applications to Southeastern Vermont," Am. Mineral. **75**, 89–96 (1990).
15. T. Holland and J. Blundy, "Non-Ideal Interactions in Calcic Amphiboles and Their Bearing on Amphibole–Plagioclase Thermometry," Contrib. Mineral. Petrol. **116**, 433–447 (1994).
16. H. Downes, P. Peltonen, I. Manttari, and E. V. Sharkov, "Proterozoic Zircon Ages from Lower Crustal Granulite Xenoliths, Kola Peninsula, Russia: Evidence for Crustal Growth and Reworking," J. Geol. Soc. (London) **159**, 485–488 (2002).